Chemical Engineering Journal 185–186 (2012) 100–107

Contents lists available at SciVerse ScienceDirect

Chemical Engineering Journal

journal homepage: www.elsevier.com/locate/cej

Copper (II) removal by pectin–iron oxide magnetic nanocomposite adsorbent

Ji-Lai Gong[a,b,*], Xi-Yang Wang[a,b], Guang-Ming Zeng[a,b], Long Chen[a,b], Jiu-Hua Deng[a,b], Xiu-Rong Zhang[a,b], Qiu-Ya Niu[a,b]

[a] College of Environmental Science and Engineering, Hunan University, Changsha 410082, PR China
[b] Key Laboratory of Environmental Biology and Pollution Control, Hunan University, Ministry of Education, Changsha 410082, PR China

ARTICLE INFO

Article history:
Received 7 November 2011
Received in revised form 7 January 2012
Accepted 9 January 2012

Keywords:
Nanocomposite
Magnetic
Pectin
Adsorption
Copper ions

ABSTRACT

This study describes an effective copper removal method using pectin-coated iron oxide magnetic nanocomposite as an adsorbent. The nanocomposite adsorbent was synthesized with the iron salt co-precipitation method followed by direct encapsulation with pectin coating without cross linking with calcium ions. Scanning electron microscopy (SEM) images showed pectin–iron oxide magnetic nanocomposite (PIOMN) adsorbent was spherical in shape and 77 ± 5 nm in diameter. Fourier transform infrared spectroscopy (FTIR) spectra provided the evidence that pectin was successfully coated on the surface of iron oxide nanoparticle. The interaction between copper ions and pectin on PIOMN surface was elucidated from energy dispersive analysis system of X-ray (EDAX) spectra. The amount of adsorbed Cu(II) by PIOMN adsorbent increased with increasing pH, followed by decreased pH value after copper uptake, attesting to the ion exchange and electrostatic force mechanism during the adsorption process. Sorption kinetic data were well fitted with a pseudo second-order model, and sorption isotherms were described by both Langmuir and Freundlich equation with maximum adsorption capacity of 48.99 mg/g. Furthermore, the adsorbents can be regenerated using 0.01 M EDTA, remaining 93.70% of its original capacity after the first regeneration cycle, and still reaching 58.66% of the original capacity after the fifth cycle.
© 2012 Elsevier B.V. All rights reserved.

1. Introduction

Copper (Cu) exists in the environment as an essential micronutrient for plants, animals and humans, particularly for plant growth [1]. The normal Cu concentration in plants reported was 4–15 mg/kg and concentration of Cu greater than 25 mg/kg was considered toxic to plants [2]. A Cu deficiency will lead to the reduction of biological functions, whereas excess Cu will damage cell membranes and result in plant cell death, thus reducing plant cover and growth, and deteriorating ecosystem [3,4]. Mining activities and the wide use of Cu-based pesticides, such as copper hydroxide and copper sulfate, for controlling fungi, bacteria, invertebrates and algae, have been cited as the leading causes of Cu toxicity to plants and soil contamination [1,5].

Much effort has been devoted to developing techniques for copper removal involving chemical precipitation, ion-exchange, membrane filtration, coagulation–flocculation, flotation, electrochemical methods and adsorption [6–12]. Among these methods, adsorption has been extensively studied as a cost-effective technology during the past decade [13,14]. Since biological material with various functional groups including carboxyl, amide and hydroxyl group, has a high affinity for Cu, various biosorbents, such as wheat [15], orange peel [16], and hardwood and corn straw [17], have been employed for Cu sorption. Pectin presenting within all higher plant cell walls is a structural polysaccharide with partially esterified polygalacturonic acid (PGA) [18]. The Cu–pectin interaction was attributed to the complexation of PGA with Cu(II) [19], for example, ML complex or ML_2 complex depending on the ligand concentration, L to M concentration ratio, and the esterified fraction [18]. As a result, pectin can be used as a biosorbent to remove Cu(II) from aqueous solution. Kartel et al. utilized industrially manufactured pectins to bind heavy metal ions in aqueous solutions and concluded that the selectivity sequences for pectins can be ordered as follows: Pb(II) ≫ Cu(II) > Co(II) > Ni(II) ≫ Zn(II) > Cd(II) [20]. Mata et al. studied the adsorption behavior of Cu, Pb and Cd from wastewater toward sugar-beet pulp pectin [21], and also investigated the sugar-beet pectin xerogels as a biosorbent for copper removal in a fixed-bed column [22]. Liang et al. utilized orange peel (OP) [16] as raw material to prepare two kinds of adsorbents, i.e., MgOP and KOP, and found that Cu(II) adsorption capacity by MgOP and KOP were 40.37 and 59.77 mg/g, respectively.

However, lack of stability and inconvenience to be separated from the aqueous solution are the main drawbacks for pectin as an

* Corresponding author at: College of Environmental Science and Engineering, Hunan University, Changsha, 410082, PR China. Tel.: +86 731 88822829; fax: +86 731 88822829.
E-mail addresses: jilaigong@gmail.com (J.-L. Gong), zgming@hnu.edu.cn (G.-M. Zeng).

1385-8947/$ – see front matter © 2012 Elsevier B.V. All rights reserved.
doi:10.1016/j.cej.2012.01.050

adsorbent for Cu(II) removal. The hybrid nanomaterials of pectin and iron oxide magnetic nanoparticles have been reported [23]. These nanomaterials have the advantages of adsorption properties of pectin and magnetic properties of iron oxide. Co-precipitation method followed by its encapsulation with pectin and cross linking with calcium ions have been employed to produce pectin coated iron oxide magnetic nanostructure hybrid [23]. A binding method using glutaraldehyde and adipic acid has been also used to synthesize pectin iron oxide magnetic nanocomposite [24]. The adsorption behavior of pectin–iron oxide magnetic adsorbent has been investigated for the removal of methylene blue from aqueous solution [24].

This paper presents a technique for producing a biological material-based magnetic adsorbent, and demonstrates highly effective Cu(II) removal by using pectin–iron oxide magnetic nanocomposite (PIOMN) adsorbent. The aim of the study is to report PIOMN synthesis and characterization, and to assess copper removal efficiency for Cu(II) from aqueous solution.

2. Materials and methods

2.1. Materials

Pectin was purchased from Sanland-chem International Inc. $FeCl_2{\cdot}4H_2O$, $FeCl_3{\cdot}6H_2O$, and $Cu(NO_3)_2\cdot 3H_2O$ were supplied by Tianjin kermel chemical reagent Co., LTD. All reagents were of chemical grade. Cu(II) stock solutions (1000 mg/L) were prepared by dissolving 3.7813 g $Cu(NO_3)_2\cdot 3H_2O$ in 1000 mL distilled water. The solutions with different concentrations were obtained by dilution of the stock solutions.

2.2. Preparation of PIOMN adsorbent

The synthesis of PIOMN was performed with the modification of the previous literatures [23,25]. Typically, iron salt co-precipitation method was used followed by direct encapsulation with pectin coating without cross linking with calcium ions. Firstly, 1% (w/v) pectin solution was prepared by dissolving 1 g pectin in 100 mL ultrapure water with continuously stirring for 24 h at room temperature. Secondly, 6.1278 g $FeCl_3\cdot 6H_2O$ and 3.0121 g $FeCl_2\cdot 4H_2O$ (molar ratio of Fe(III): Fe(II) was 1.5: 1) were dissolved in 100 mL ultrapure water and heated to 90 °C with N_2 protection, followed by rapid addition of 10 mL of 25 wt % ammonium hydroxide, with subsequent addition of 100 mL of prepared pectin solution. Finally, the mixture was stirred at 90 °C for 30 min and then cooled to room temperature. After reaction, the black precipitate was collected by a permanent magnet, washed with copious distilled water to neutral, dried in the oven at 90 °C, and grinded with mortar. The final products were the prepared PIOMN adsorbents.

2.3. Sample analysis methods

FTIR spectra of bare Fe_3O_4 nanoparticles and PIOMN before and after Cu(II) uptake were recorded with a Fourier Transform Infrared Spectroscopy (FTIR, WQF-410, Beijing Second Optical Instrument Factory, China). The size and morphology of the synthesized PIOMN was characterized by scanning electron microscopy (SEM) analysis using a JSM-5600 LV microscope (JEO, Ltd., Japan). The sample composition and element contents were analyzed by energy dispersive analysis system of X-ray (EDAX) using an EDX-GENESIS (EDAX, Ltd., USA). The Brunauer–Emmett–Teller (BET) specific surface area was determined by ASAP 2020 Accelerated Surface Area and Porosimetry System (Micromeritics Instrument Corporation; USA). The zeta potential of PIOMN suspensions was measured using a Zeta Meter 3.0 (Zeta Meter Inc.) equipped with a microprocessor unit. The magnetic properties were characterized by magnetization curves using a HH-50 vibrating sample magnetometer in the condition of sensitivity 20 mV.

2.4. Adsorption experiments

All batch experiments were carried out on a constant temperature bath oscillator to vibrate at room temperature (25 ± 1 °C) at 120 rpm. The designed solution pH was adjusted using 0.1 M NaOH or HCl. After reaction, the PIOMN were separated from the solutions using a permanent magnet, and the initial and final metal concentrations were determined by a Perkin-Elmer Analyst 700 AAS. The equilibrium adsorption capacity (q_e) was calculated according to the following equation,

$$q_e = \frac{(C_0 - C_e)V}{W} \quad (1)$$

where q_e is the equilibrium adsorption capacity (mg/g), C_0 and C_e are the initial and equilibrium liquid phase solute concentration (mg/L), respectively, V is the liquid phase volume (L) and W is the amount of adsorbent (g).

2.4.1. Kinetic experiments

Batch kinetic tests were conducted by mixing 150 mg PIOMN adsorbents with 150 mL of Cu(II) aqueous solution with concentration of 100 mg/L at pH 5.00 ± 0.10 in 250 mL flasks. Then, the flasks were put on a constant temperature bath oscillator to vibrate. Samples were withdrawn at preselected time intervals ranging from 5 min to 2 days and the residual metal concentrations were determined after magnetic separation.

2.4.2. Isotherms

Sorption isotherms were performed by mixing 20 mg PIOMN adsorbents with 20 mL metal solutions with different initial concentrations ranging from 10 mg/L to 1000 mg/L followed by adjusting the solution pH to 5.00 ± 0.10. Then the flasks were put on a constant temperature bath oscillator to vibrate for 24 h. After reaction and subsequent separation, the final metal concentrations in supernatant were measured.

2.4.3. Effect of PIOMN dosage

To investigate the effect of adsorbent dosage on the adsorption capacity, 20 mL of 100 mg/L Cu(II) solution were adjusted to pH 5.00 ± 0.10 in flasks, followed by addition of various amount of adsorbents. After 24 h and magnetic separation, the residual metal concentrations were analyzed.

2.4.4. Effect of pH

The effect of pH on adsorption capacity was conducted by mixing 20 mg PIOMN adsorbents with 20 mL of 100 mg/L Cu(II) aqueous solution with different pH value ranging from 2.16 to 5.73 under vibrating condition for 24 h in oscillating water bath shaker. After reaction and followed by magnetic separation, the residual metal concentrations were determined.

2.4.5. Effect of ionic strength

To investigate the effect of ionic strength on adsorption capacity, $NaNO_3$ and $Ca(NO_3)_2$ with concentrations ranging from 0 to 0.2 mol/L were added to 100 mg/L Cu(II) solution at pH 5.00 ± 0.10 with the adsorbents dose of 1 g/L under vibrating condition for 24 h in oscillating water bath shaker. After reaction and subsequent magnetic separation, the residual metal concentrations were determined.

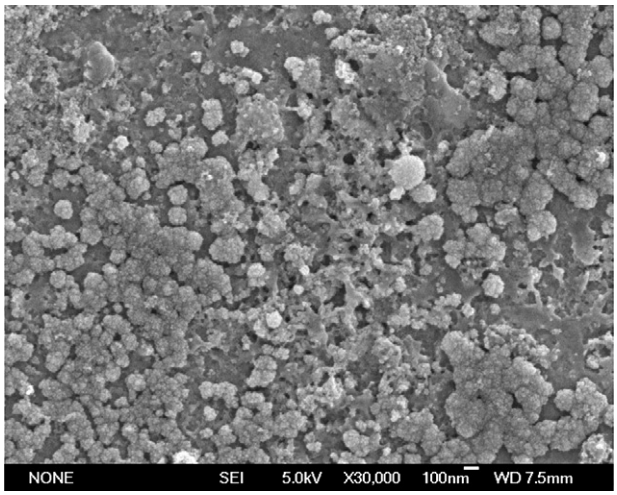

Fig. 1. SEM micrograph of PIOMN.

2.5. Desorption and reusability

Desorption experiments were investigated using different solutions involving EDTA, HCl, and NaOH. PIOMN adsorbent was first loaded with Cu(II) by mixing 20 mg adsorbent with 20 mL of 100 mg/L Cu(II) solution to vibrate for 24 h to reach equilibrium. The resultant suspensions were magnetically separated and the final concentration of Cu(II) adsorbed on PIOMN adsorbent was determined. Subsequently, the solid residue was thoroughly washed with copious distilled water and mixed with 20 mL of various eluants including EDTA, HCl, and NaOH at room temperature ($25 \pm 1\,^{\circ}C$) under vibrating condition for 24 h. After reaction and subsequent magnetic separation, the remaining Cu(II) concentration in supernatant was measured.

3. Results and discussion

3.1. Characterization of PIOMN adsorbents

Fig. 1 showed the physical properties of the PIOMN adsorbents, including their morphologies and sizes. SEM image revealed that PIOMN adsorbents are nearly spherical in shape and 77 ± 5 nm in diameter, and tend to agglomerate into larger aggregates, resulting in a rough surface and porous structure. It was noted that the BET specific surface area of PIOMN adsorbents was 67.00 m^2/g.

Infra red spectra were collected to investigate whether pectin biomaterials bound to iron oxide nanoparticles and the Cu(II) adsorption behavior. Many additional peaks occurred after pectin binding to iron oxide nanoparticles, whereas few peaks appeared in iron oxide nanoparticles without pectin coating, thus elucidating the successful binding of pectin polymer on iron oxide nanoparticles (see Fig. 2(a) and (b)). The appearance of broad peak at ~3397 cm^{-1} was attributed to the O—H stretching vibrations [16] and the peak at ~580 cm^{-1} in both iron oxide nanoparticles and PIOMN adsorbents was resulted from the stretching vibration of Fe—O—Fe in Fe_3O_4 [26]. For PIOMN adsorbents alone, the peak at 1736 cm^{-1} was assigned to the C=O stretches in free carboxylic acid [27]. The peaks at 1603 cm^{-1} and 1402 cm^{-1} may be caused by asymmetric and symmetric stretching vibrations of carboxylic acids in ionic form ($—COO^-$), respectively [28], and the peak at 1095 cm^{-1} indicated the stretching vibration of C—OH of alcoholic groups and carboxylic acids. The band at 1016 cm^{-1} may be due to the vibrations associated with the skeletal rings of the sugar monomers of pectin [28]. Noticeably, the peak at 1736 cm^{-1} disappeared after PIOMN adsorbents uptake

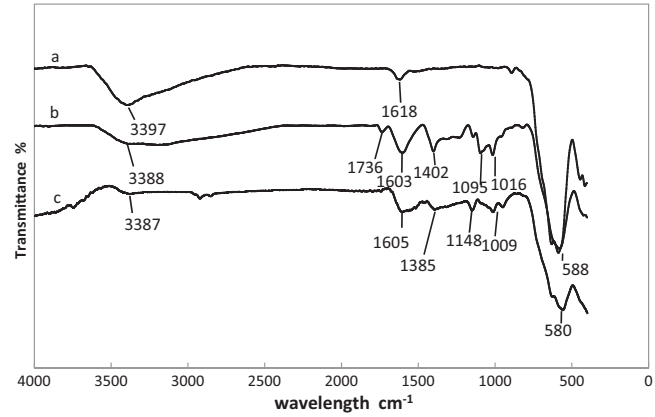

Fig. 2. FTIR spectra of Fe_3O_4 nanoparticles (a), FTIR spectra of PIOMN before loading Cu(II) (b) and FTIR spectra of PIOMN after loading Cu(II) (c).

of Cu(II) (Fig. 2(c)). It was documented that, one of the mechanism of pectin bounding heavy metal is ion exchange [20,29]. Thus, the disappearance of peak at 1736 cm^{-1} after copper uptake in PIOMN can be explained that Cu(II) substituted the H(I) of —COOH and formed —COO—Cu complexation, confirming the ion exchange mechanism. On the other hand, the measurable changes in the peaks of the FTIR spectra at 1603 cm^{-1} and 1402 cm^{-1}

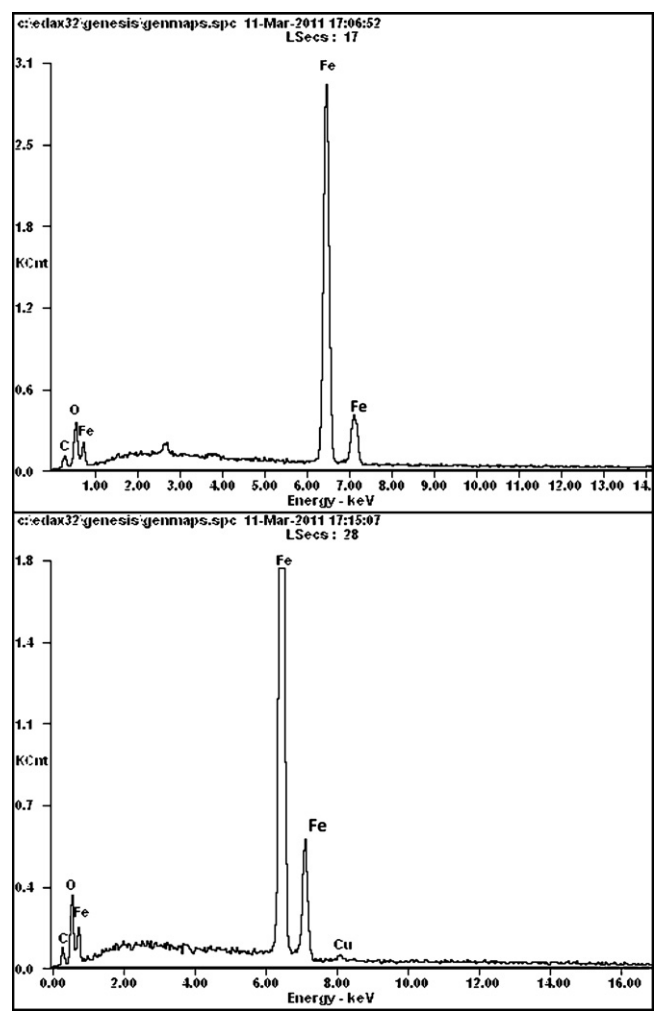

Fig. 3. EDAX spectra of PIOMN before and after loading Cu (II).

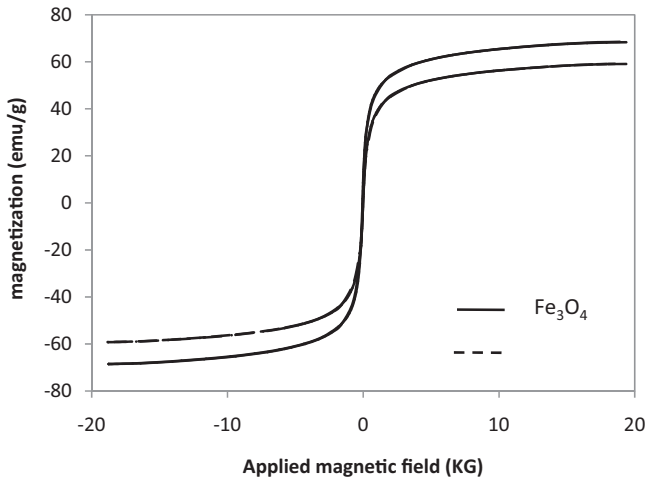

Fig. 4. Magnetization curves of Fe_3O_4 nanoparticles and PIOMN.

may be due to the electrostatic interaction between Cu(II) and $-COO^-$.

EDAX spectra of PIOMN adsorbents were collected before and after copper uptake (see Fig. 3). Results showed that copper peak was absent for PIOMN adsorbents alone, but observable copper peak was obtained while PIOMN adsorbents were laden with Cu(II), confirming the successful copper loading on the surface of PIOMN.

The measured saturation magnetization of PIOMN adsorbent was 59.2 emu/g (depicted in Fig. 4), which was slightly less than bare iron oxide nanoparticles (68.5 emu/g), but it was high enough to separate from aqueous solution because saturation magnetization of 16.3 emu/g was sufficient for magnetic separation with a conventional permanent magnet [30].

3.2. Adsorption kinetics

Results of sorption kinetics presented in Fig. 5(a) suggested that Cu(II) removal mainly took place within the first 2 h, followed by a slow increase of adsorption until the equilibrium was reached. In order to investigate sorption kinetics, pseudo-first-order, pseudo-second-order, and intra-particle diffusion models were applied to fit our experimental data. A pseudo-first-order kinetic model is given as the following equation,

$$\log(q_e - q_t) = \log q_e - \frac{k_1 t}{2.303} \quad (2)$$

A pseudo-second-order kinetic model is also analyzed to fit the data and given by,

$$\frac{t}{q_t} = \frac{1}{k_2 q_e^2} + \frac{t}{q_t} \quad (3)$$

The intra-particle diffusion model equation is,

$$q_e = k_p t^{0.5} + C \quad (4)$$

where q_e and q_t are the amounts of metal ions adsorbed on per unit PIOMN at equilibrium and at time t, respectively (mg/g), k_1 is the pseudo-first-order rate constant for the adsorption process and can be obtained from the plots of $\log(q_e - q_t)$ against t, k_2 is the pseudo-second-order rate constant for the adsorption process and can be calculated from the plots of t/q_t against t, k_p is the intra-particle diffusion rate constant and can be obtained from the slope of straight-line portions of plot of q_t against $t^{0.5}$, and C is a constant gained from the intercept of plot of q_t against $t^{0.5}$.

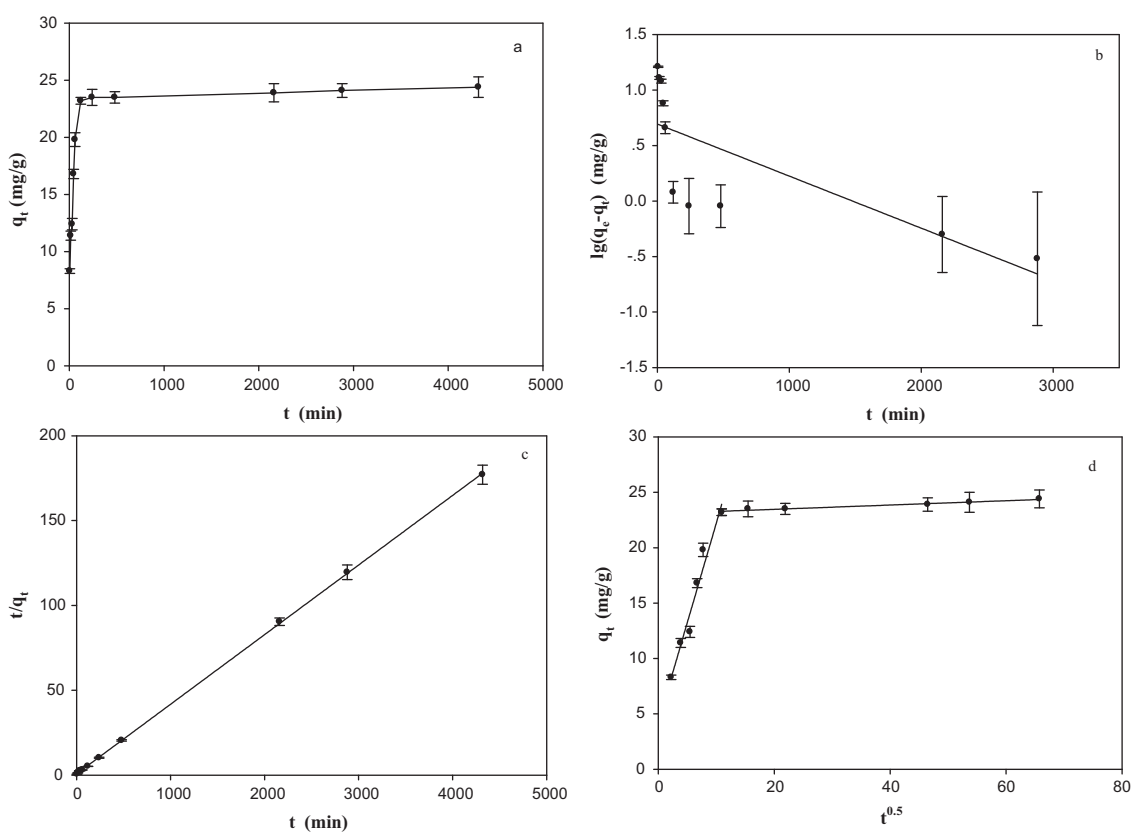

Fig. 5. The influence of contact time on the amount of Cu(II) absorption by PIOMN(a), the pseudo-first-order kinetic model (b), the pseudo-second-order kinetic model (c), and intra-particle diffusion plots (d) for Cu(II) adsorption by PIOMN. (volume, 150 mL; absorbent dose, 150 mg; initial concentration, 100 mg/L; pH, 5.00 ± 0.10; contact time, 0 min, 5 min, 15 min, 30 min, 45 min, 1 h, 2 h, 4 h, 8 h, 24 h, 36 h, 48 h 72 h; temperature, 25 ± 1 °C; agitation speed, 120 rpm.)

Table 1
Kinetic parameters for Cu(II) adsorption onto PIOMN.

Pseudo-first-order	Pseudo-second-order	Intra-particle diffusion
$q_{e,exp}$ = 24.40 mg/g		
$q_{e,cal}$ = 4.94 mg/g	$q_{e,cal}$ = 24.33 mg/g	k_p = 1.7955 mg $h^{0.5}$/g
k_1 = 0.0012 h^{-1}	k_2 = 0.0016 g/(mg h)	R^2 = 0.9597
R^2 = 0.5635	R^2 = 0.9992	

Table 2
Isotherm constants for Cu(II) adsorption onto PIOMN.

Langmuir model	Freundlich model
q_{max} = 48.99 mg/g	K_F = 5.4601 mg/[g (mg/L)$^{1/n}$]
b = 0.0103 L/mg	$1/n$ = 0.3179
R^2 = 0.9799	R^2 = 0.9881

The results of linear forms of pseudo-first-order, pseudo-second-order and intra-particle diffusion kinetic models on the experiment data were presented in Fig. 5. Table 1 lists the kinetic parameters for Cu(II) removal by PIOMN adsorbents using pseudo-first-order, pseudo-second-order, and intra-particle diffusion models. A linear relationship with high correlation coefficient (R^2 = 0.9992) (given in Table 1) between t/q_t and t was obtained, indicating the applicability of the pseudo-second-order model to better describe the adsorption process than pseudo first-order model (R^2 = 0.5635). Therefore the rate-limiting step for removal Cu(II) by PIOMN adsorbent may be caused by chemical adsorption [31].

It was noticed that two straight lines with different slopes can be found in the linear of q_e against $t^{0.5}$ (Fig. 5(d)) revealing that the adsorption process was obviously divided into two steps. The first linear step was a very fast stage due to the boundary layer effect, followed by the intra-particle diffusion step. Results showed that the intraparticle diffusion was not the rate-controlling step because it did not pass through the origin.

3.3. Adsorption isotherms

In order to determine the sorption capacity of PIOMN adsorbent toward Cu(II), sorption studies with initial concentrations ranging from 10 to 1000 mg/L were carried out. The equilibrium isotherms for Cu(II) adsorption were given in Fig. 6. The two common adsorption models involving Langmuir model and Freundlich model are widely used to describe the adsorption behavior. The Langmuir equation is,

$$\frac{1}{q_e} = \frac{1}{q_m b C_e} + \frac{1}{q_m} \quad (5)$$

where q_e is the equilibrium adsorption capacity of adsorbent toward Cu(II) (mg/g), C_e is the equilibrium Cu(II) concentration in solution (mg/L), q_m is the maximum capacity of adsorbent (mg/g), and b is the Langmuir adsorption constant pertaining to the energy of adsorption (L/mg). The linear form of Freundlich equation, an empirical equation used to describe heterogeneous adsorption systems, can be represented by the following equation,

$$\ln q_e = \ln K_F + \frac{1}{n} \ln C_e \quad (6)$$

where q_e and C_e are defined as above, K_F is Freundlich constant (L/mg), and n is the heterogeneity factor. The values of q_m and b were calculated by the slope and intercept of the linear plot of $1/q_e$ versus $1/C_e$, and the values of K_F and $1/n$ were obtained from the slope and intercept of the linear plot of ln q_e versus ln C_e. Table 2 lists the correlation coefficients of Langmuir and Freundlich isotherms, i.e., 0.9799 and 0.9881, respectively, thus revealing that the data were well fitted both Freundlich and Langmuir equation, and slightly better described by Freundlich isotherm. The adsorption capacity of PIOMN toward Cu(II) was about 48.99 mg/g according to Langmuir isotherm data. Noticeably, the pectin concentration during the process of PIMON synthesis was the key parameter to achieve suitable size distribution and optimal adsorption capacity of the obtained nanostructures. Actually, we also prepared PIMON nanostructures using pectin solution at different concentrations (i.e., 0.5%, 1.5% and 2.0% (w/v)). Results show that the diameter of PIOMN adsorbents were around 30 ± 4 nm, 80 ± 5 nm and 84 ± 10 nm for the PIOMN adsorbents prepared using 0.5%, 1.5% and 2.0% pectin, respectively (displayed in Fig. S1 in supporting information). Additionally, the prepared PIOMN adsorbents tended to agglomerate into larger aggregates and showed reduced saturation magnetization with increasing concentration of pectin added during synthesis (see Figure S1 and S2 in supporting information). We also found that the adsorption capacities of PIMON nanostructures were 46.19 mg/g, 39.73 mg/g and 38.66 mg/g for the PIOMN adsorbents prepared using 0.5%, 1.5% and 2.0% pectin, respectively (given in Figure S3 and Table S1 in supporting information). The reason could be due to their different specific surface areas and pectin contents. The specific surface area was 66.85 m^2/g and 12.19 m^2/g for the PIOMN adsorbents prepared using 1.5% and 2.0% pectin, respectively, which were smaller than that prepared using 1% pectin (67.00 m^2/g), thus demonstrating their lower adsorption capacities. Although the specific surface area of PIOMN adsorbent prepared using 0.5% pectin (84.97 m^2/g) was larger than that prepared using 1% pectin, its adsorption capacity was relatively lower because of its less content of pectin. Therefore, PIOMN adsorbent prepared using 1.0% (w/v) pectin showed the best behavior in terms of particle size distribution and adsorption capacity and was resultantly selected in this work during the synthesis of PIMON nanostructure adsorbents. However, the amount of Cu(II) adsorbed by bare iron oxide nanopartlcles was only about 11.00 mg/g under the same condition. As a consequence, PIOMN adsorbent was much more effective in Cu(II) removal than bare iron oxide nanopartlcles, confirming that pectin-coated iron oxide nanoparticles greatly enhanced Cu(II) removal efficiency from aqueous solution. In addition, the maximum adsorption capacity of PIOMN toward Cu(II) (48.99 mg/g) was much higher than previous reported adsorbents, such as collagen–tannin resin (17.02 mg/g) [32], Carboxymethylated-bacterial cellulose (12.63 mg/g) [33]. It was noted that the PIOMN adsorption capacity for Cu(II) in this work was comparable to pectin-containing natural material, such as the ionic treated orange peel (40.37 mg/g for MgOP; 59.77 mg/g for KOP) [16], and sugar-beet pectin xerogels (from 34.80 to

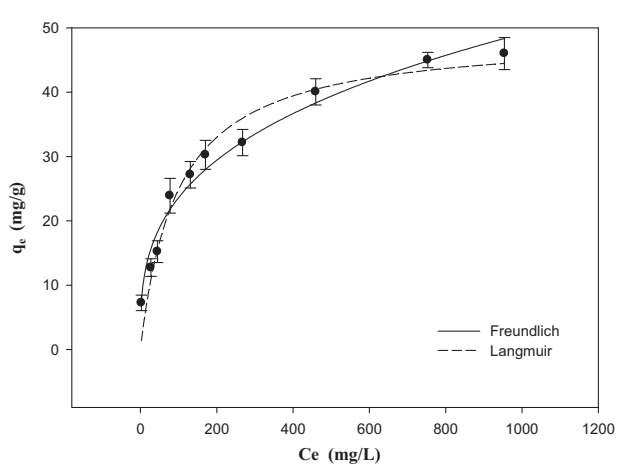

Fig. 6. Adsorption isotherm of Cu(II) adsorbed by PIOMN. (volume, 20 mL; absorbent dose, 20 mg; initial concentration, 10–1000 mg/L; contact time, 24 h; pH = 5.00 ± 0.10; temperature, 25 ± 1 °C; agitation speed, 120 rpm.)

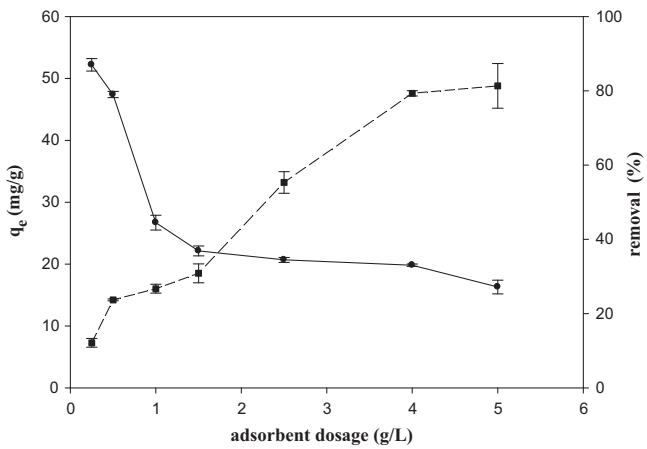

Fig. 7. The relationship between PIOMN dosage and Cu(II) adsorbed by PIOMN. (volume, 20 mL; absorbent dose, 5 mg; 10 mg; 20 mg; 30 mg; 50 mg; 80 mg; 100 mg, initial concentration, 100 mg/L; contact time, 24 h; pH, 5.00 ± 0.10; temperature, 25 ± 1 °C; agitation speed, 120 rpm.)

58.00 mg/g depending on adsorbent dosage) [21]. However, the pectin-rich natural materials as adsorbents suffered from low stability and separation inconvenience.

3.4. Effect of PIOMN dosage

The plot of PIOMN amount versus the Cu(II) adsorption quantities (Fig. 7) revealed that the percentage of Cu(II) adsorbed by PIOMN increased with increasing adsorbent load. Conversely, the adsorption amount per unit of adsorbent decreased with increasing PIOMN amount. This observation can be explained that the number of available adsorption sites increased by increasing adsorbent dose, resulting in the increase of adsorbed Cu(II) amount, while unsaturation of adsorption sites through the adsorption process contributed to the decrease in equilibrium uptake with increasing adsorbent dose.

3.5. Effect of pH

The effect of solution pH on Cu(II) uptake by PIOMN was investigated at pH values ranging from 2.16 to 5.73. The amount of Cu(II) adsorbed on PIOMN increased with increasing pH value (Table 3). Results of PIOMN zeta potential at different pH values ranging from 2.07 to 9.25 (Fig. 8), elucidated that the isoelectric point of the adsorbent was about 2.50, and that the charge sign on the surface of PIOMN adsorbents was positive at pH < 2.50, and negative at pH > 2.50, with the higher pH value, the higher negative charge density on PIOMN surface. Therefore, Cu(II) removal was suppressed at lower pH value, possibly resulting from a competition between hydrogen and metal ions toward sorption sites. In contrast, Cu(II) removal was enhanced at higher pH value, due to the increasing negative charge density on PIOMN surface, leading to the increased adsorption of Cu(II). Thus, considering the evidence of FTIR, we demonstrated that adsorption process in this work was

Table 3
Effect of initial pH on Cu(II) adsorption onto PIOMN.

Initial pH	Final pH	q_e (mg/g)	$q_{ion\text{-}exchange}$ (mg/g)	$q_{ion\text{-}exchange}/q_e$ (%)
2.16	2.15	10.50	5.16	49.14
3.08	2.95	18.30	9.29	50.77
4.02	3.25	21.30	14.94	70.14
4.88	3.31	26.00	15.25	58.65
5.73	3.80	29.40	15.01	51.05

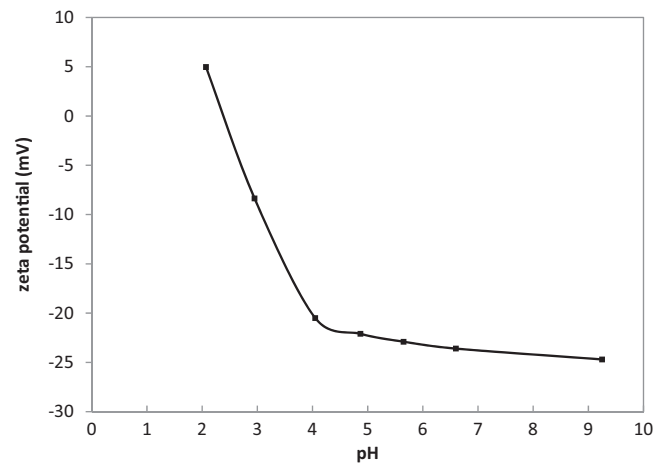

Fig. 8. Zeta potentials of PIOMN at various pH values.

partly attributed to electrostatic attraction. It was noted that the pH value was ≤5.73 due to the formation of precipitation between Cu(II) and too much hydroxyl ions.

It was noted that the solution pH value after PIOMN adsorbent uptake of Cu(II) is lower than brfore (Table 3), which was caused by release of H(I) from PIOMN adsorbent surface, resultantly elucidating ion exchange mechanism during Cu(II) adsorption process between Cu(II) and H(I) of carboxyl acid on PIOMN surface.

3.6. Effect of ionic strength on Cu(II) adsorption

To investigate ionic strength effects on Cu(II) removal by PIOMN adsorbent, sodium chloride and calcium chloride with varying concentrations were used (Fig. 9). The results showed a trend that an increase in salt concentrations resulted in a decrease in Cu(II) uptake by PIOMN. This trend indicated that the Cu(II) binding efficiency on PIOMN adsorbent decreased when salt concentrations increased in the presence of Cu(II), which was attributed to the competition between Cu(II) and cations involving Na(I) and Ca(II) for available sites during sorption process. Additionally, the trend also indicated that the salt effect on Cu(II) toward PIOMN caused by Ca(II) was more noticeable than Na(I), probably derived from the same charge sign between Ca(II) and Cu(II).

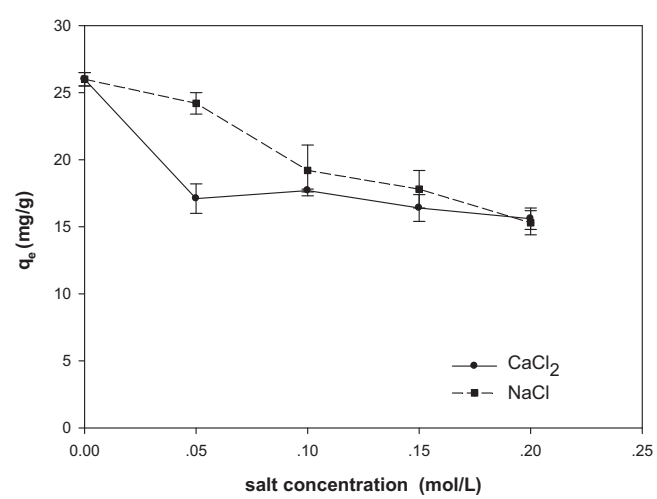

Fig. 9. Effect of salt concentration on adsorption of Cu(II) by PIOMN (volume, 20 mL; absorbent dose,20 mg, initial concentration, 100 mg/L; contact time, 24 h; pH, 5.00 ± 0.10; temperature, 25 ± 1 °C; agitation speed, 120 rpm, salt concentration, 0-0.2 mol/L).

Table 4
Desorption of Cu(II) from loaded PIOMN.

Eluant	Concentration (mol/L)	Desorbed (%)
EDTA	0.01	93.22
HNO_3	0.1	59.61
NaOH	0.1	0

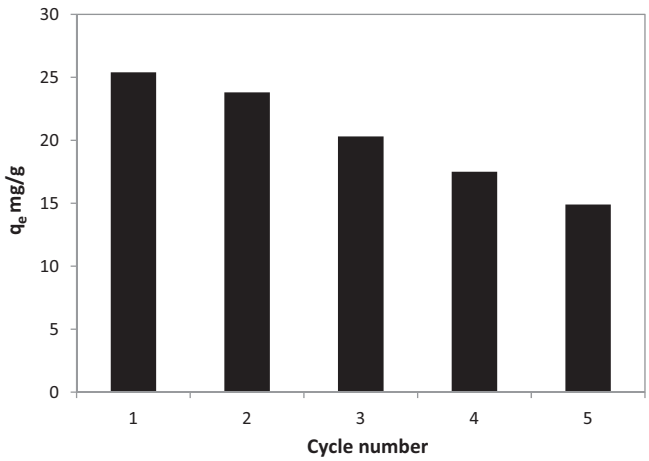

Fig. 10. Reusability of PIOMN regenerated by 0.01 M EDTA. (Adsorption: volume, 20 mL; absorbent dose, 20 mg, initial concentration, 100 mg/L; contact time, 24 h; pH, 5.00 ± 0.10; temperature, 25 ± 1 °C; agitation speed, 120 rpm. Desorption: volume, 20 mL; absorbent dose, 20 mg; contact time, 24 h; temperature, 25 ± 1 °C; agitation speed, 120 rpm.)

3.7. Desorption and reusability

Desorption behavior was studied using 0.01 M EDTA, 0.1 M HNO_3, and 0.1 M NaOH as eluants (listed in Table 4). Results showed that desorption percentages for Cu(II) by 0.01 M EDTA and 0.1 M HNO_3 were 93.70% and 59.61%, respectively. However, the amount of metal ions desorbed from 0.1 M NaOH was negligible, indicating relatively high stability of adsorbed Cu(II) on PIOMN under alkaline conditions, which was in accord with result described above that adsorption capacity of PIOMN increased at higher pH. Thus, the optimum eluant for desorption Cu(II) from PIOMN adsorbent was 0.01 M EDTA derived from the formation of complex between EDTA and Cu(II). As a consequence, 0.01 M EDTA was selected to investigate the reusability of PIOMN adsorbent for Cu(II) removal. Fig. 10 depicted the relationship between regeneration cycle numbers and adsorption capacity of PIOMN. The value of cycle 0 was denoted as the adsorption capacity of the original PIOMN. Obviously, the adsorption capacity decreased with increasing regeneration cycle numbers, remained 93.70% of its original capacity after the first regeneration cycle, and still reached 58.66% of the original capacity after the fifth cycle, resultantly, exhibiting good regeneration results and showing promise for reusability of PIOMN adsorbent for Cu(II) removal.

4. Conclusions

In this study, the preparation and adsorption potential of PIOMN was investigated for the removal of Cu (II) from aqueous systems. The system has been optimized to achieve suitable size distribution of the obtained PIOMN. The effects of contact time, initial Cu (II) concentrations, pH, adsorbent dosage and ions strength on the adsorption process and desorption were discussed. FTIR spectra elucidated the successful pectin coating on iron oxide nanoparticles surface. EDAX analysis provided the evidence for Cu(II) uptake by PIOMN adsorbent. Adsorption kinetics was fitted with the pseudo-second-order model, and adsorption isotherms were described by both Freundlich and Langmuir equation with maximum adsorption capacity of 48.99 mg/g. The adsorption mechanism of Cu(II) uptake in PIOMN adsorbent was based on ion exchange between hydrogen ions of free carboxylic acid in PIOMN adsorbent and copper ions in solution, and electrostatic force between Cu(II) and PIOMN adsorbent. Increasing salt concentration resulted in a decrease in Cu(II) uptake by PIOMN. Desorption experiments demonstrated that 0.01 M EDTA was an efficient eluant with 93.70% of Cu(II) released from PIOMN for the first regeneration cycle and 58.66% for the fifth cycle. In conclusion, PIOMN is a promising alternative for Cu(II) removal from wastewater because of its high adsorption capacity and separation convenience.

Acknowledgments

The authors are grateful for the financial supports from National Natural science Foundation of China (50808070, 51039001), the program for New Century Excellent Talents in University from the Ministry of Education of China (NCET-09-0328), the Postdoctoral Science Foundation of China (20070410301, 200902468), the Program for Changjiang Scholars and Innovative Research Team in University (IRT0719), Hunan Provincial Natural Science Foundation of China (08JJ4006, 10JJ7005), the Xiangjiang Water Environmental Pollution Control Project subjected to the National Key Science and Technology Project for Water Environmental Pollution Control (2009ZX07212-001-02 and 2009ZX07212-001-06), and the Hunan Key Scientific Research Project (2009FJ1010).

Appendix A. Supplementary data

Supplementary data associated with this article can be found, in the online version, at doi:10.1016/j.cej.2012.01.050.

References

[1] K.W. Juang, H.Y. Lai, B.C. Chen, Coupling bioaccumulation and phytotoxicity to predict copper removal by switchgrass grown hydroponically, Ecotoxicology 20 (2011) 827–835.
[2] D. Gjorgieva, T.K. Panovska, K. Baceva, T. Stafilov, Assessment of heavy metal pollution in republic of macedonia using a plant assay, Arch. Environ. Contam. Toxicol. 60 (2011) 233–240.
[3] J. Kovacik, J. Gruz, M. Backor, J. Tomko, M. Strnad, M. Repcak, Phenolic compounds composition and physiological attributes of Matricaria chamomilla grown in copper excess, Environ. Exp. Bot. 62 (2008) 145–152.
[4] S. Meiera, R. Azcónb, P. Cartesa, F. Boriea, P. Cornejoa, Alleviation of Cu toxicity in *Oenothera picensis* by copper-adapted arbuscular mycorrhizal fungi and treated agrowaste residue, Appl. Soil Ecol. 48 (2011) 117–124.
[5] G.Y. Guo, T. Yuan, W.H. Wang, D. Li, J.P. Cheng, Y. Gao, P. Zhou, Bioavailability, mobility, and toxicity of Cu in soils around the Dexing Cu mine in China, Environ. Geochem. Health 33 (2011) 217–224.
[6] Q.Y. Chen, Z. Luo, C. Hills, G. Xue, M. Tyrerc, Precipitation of heavy metals from wastewater using simulated flue gas: sequent additions of fly ash, lime and carbon dioxide, Water Res. 43 (2009) 2605–2614.
[7] A.C. Alvarez, A.H. Gonzalez, N. Casillas, R.P. Ramirez, M.E. Espinosa, V. Soto, W. de la Cruz, M.B. Soto, S.G. Salazar, Cu (II) removal from tequila using an ion-exchange resin, Food Chem. 127 (2011) 1503–1509.
[8] Y.M. Sang, Q.B. Gu, T.C. Sun, F.S. Li, C.Z. Liang, Filtration by a novel nanofiber membrane and alumina adsorption to remove copper(II) from groundwater, J. Hazard. Mater. 153 (2008) 860–866.
[9] J.C. Duan, Q. Lu, R.W. Chen, Y.Q. Duan, L.F. Wang, L. Gao, S.Y. Pan, Synthesis of a novel flocculant on the basis of crosslinked Konjac glucomannan-graft-polyacrylamide-co-sodium xanthate and its application in removal of Cu^{2+} ion, Carbohydr. Polym. 80 (2010) 436–441.
[10] X.Z. Yuan, Y.T. Meng, G.M. Zeng, Y.Y. Fang, J.G. Shi, Evaluation of tea-derived biosurfactant on removing heavy metal ions from dilute wastewater by ion flotation, Colloids Surf. A: Physicochem. Eng. Aspects 317 (2008) 256–261.
[11] R.S. Juang, L.C. Lin, Electrochemical treatment of copper from aqueous citrate solutions using a cation-selective membrane, Sep. Purif. Technol. 22–23 (2001) 627–635.
[12] R.P. Hana, W.H. Zou, Z.P. Zhang, J. Shi, J.J. Yang, Removal of copper(II) and lead(II) from aqueous solution by manganese oxide coated sand. I. Characterization and kinetic study, J. Hazard. Mater. B137 (2006) 384–395.

[13] B. Yu, Y. Zhang, A. Shukla, S.S. Shukla, K.L. Dorris, The removal of heavy metal from aqueous solutions by sawdust adsorption—removal of copper, J. Hazard. Mater. B80 (2000) 33–42.
[14] K.O. Adebowale, I.E. Unuabonah, B.I. Olu-Owolabi, Adsorption of some heavy metal ions on sulfate- and phosphate-modified kaolin, Appl. Clay Sci. 29 (2005) 145–148.
[15] U. Farooq, J.A. Kozinski, M.A. Khan, M. Athar, Biosorption of heavy metal ions using wheat based biosorbents—a review of the recent literature, Bioresour. Technol. 101 (2010) 5043–5053.
[16] S. Liang, X.Y. Guo, N.C. Feng, Q.H Tian, Isotherms, kinetics and thermodynamic studies of adsorption of Cu^{2+} from aqueous solutions by Mg^{2+}/K^{+} type orange peel adsorbents, J. Hazard. Mater. 174 (2010) 756–762.
[17] X.C. Chen, G.C. Chen, L.G. Chen, Y.X. Chen, J. Lehmann, M.B. McBride, A.G. Hay, Adsorption of copper and zinc by biochars produced from pyrolysis of hardwood and corn straw in aqueous solution, Bioresour. Technol. 102 (2011) 8877–8884.
[18] C. Vilhena, M.L. Goncalves, A.M. Mota, Binding of copper(II) to pectins by electrochemical methods, Electroanalytical 16 (2004) 2065–2072.
[19] A.M. Khvan, K.A. Abduazimov, Complexation in the nitrolignin–pectin–copper ion system, Chem. Nat. Compd. 37 (2001) 388–390.
[20] M.T. Kartel, L.A. Kupchik, B.K. Veisov, Evaluation of pectin binding of heavy metal ions in aqueous solutions, Chemosphere 38 (1999) 2591–2596.
[21] Y.N. Mata, M.L. Blázquez, A. Ballester, F. González, J.A. Munoz, Sugar-beet pulp pectin gels as biosorbent for heavy metals: preparation and determination of biosorption and desorption characteristics, Chem. Eng. J. 150 (2009) 289–301.
[22] Y.N. Mata, M.L. Blazquez, A. Ballester, F. Gonzalez, J.A. Munoz, Optimization of the continuous biosorption of copper with sugar-beet pectin gels, J. Environ. Manage. 90 (2009) 1737–1743.
[23] S. Sahu, R.K. Duttan, Novel hybridnanostructuredmaterials of magnetite nanoparticles and pectin, J. Magn. Magn. Mater. 323 (2011) 980–987.
[24] R. Rakhshaee, M. Panahandeh, Stabilization of a magnetic nano-adsorbent by extracted pectin to remove methylene blue from aqueous solution: a comparative studying between two kinds of cross-likened pectin, J. Hazard. Mater. 189 (2011) 158–166.
[25] M. Faraji, Y. Yamini, M. Rezaee, Magnetic nanoparticles: synthesis, stabilization, functionalization, characterization, and applications, J. Iran. Chem. Soc. 7 (2010) 1–37.
[26] T.T. Baby, S. Ramaprabhu, SiO_2 coated Fe_3O_4 magnetic nanoparticle dispersed multiwalled carbon nanotubes based amperometric glucose biosensor, Talanta 80 (2010) 2016–2022.
[27] J.F. Liu, Z. Shan, H. Zhao, G.B. Jiang, Coating Fe_3O_4 magnetic nanoparticles with humic acid for high efficient removal of heavy metals in water, Environ. Sci. Technol. 42 (2008) 6949–6954.
[28] L. Chen, R.H. Wilson, M.C. McCann, Infra-red microspectroscopy of hydrated biological systems: design and construction of a new cell with atmospheric control for the study of plant cell walls, J. Microsc. 188 (1997) 62–71.
[29] G.S. Chauhan, A. Kumari, R. Sharma, Pectin and acrylamide based hydrogels for environment management technologies: synthesis, characterization, and metal ions sorption, J. Appl. Polym. Sci. 106 (2007) 2158–2168.
[30] Z.Y. Ma, Y.P. Guan, H.Z. Liu, Synthesis and characterization of micron-sized monodisperse superparamagnetic polymer particles with amino groups, J. Appl. Polym. Sci.: Part A: Polym. Chem. 43 (2005) 3433–3439.
[31] F.C. Wu, R.L. Tseng, R.S. Juang, Enhanced abilities of highly swollen chitosan beads for color removal and tyrosinase immobilization, J. Hazard. Mater. B81 (2001) 167–177.
[32] X. Sun, X. Huang, X.P. Liao, B. Shi, Adsorptive removal of Cu(II) from aqueous solutions using collagen-tannin resin, J. Hazard. Mater. 186 (2011) 1058–1063.
[33] S.Y. Chen, Y. Zou, Z.Y. Yan, W. Shen, S.K. Shi, X. Zhang, H.P. Wang, Carboxymethylated-bacterial cellulose for copper and lead ion removal, J. Hazard. Mater. 161 (2009) 1355–1359.